Chinese Journal of Catalysis 34 (2013) 585–592

available at www.sciencedirect.com

ScienceDirect

journal homepage: www.elsevier.com/locate/chnjc

Article

La-doped titania nanocrystals with superior photocatalytic activity prepared by hydrothermal method

JIAO Yanchao, ZHU Mingfeng, CHEN Feng *, ZHANG Jinlong

Key Laboratory for Advanced Materials and Institute of Fine Chemicals, East China University of Science and Technology, Shanghai 200237, China

ARTICLE INFO

Article history:
Received 15 October 2012
Accepted 10 November 2012
Published 20 March 2013

Keywords:
Potassium octatitanate
Phase transition
La-doped titania
Photocatalytic activity
Hydrothermal synthesis

ABSTRACT

Potassium titanate (KTO) nanobars were synthesized by a hydrothermal method and used as a precursor to synthesize TiO_2 nanocrystals. La doping of the TiO_2 nanocrystals was achieved by introducing La^{3+} into the hydrothermal media. The hydrothermal transition of KTO to TiO_2 was investigated under various conditions, finding that the pH of the hydrothermal media, the temperature, and the pre-treating procedure play important roles in the phase transition. X-ray diffraction and transmission electron microscopy were used to characterize the crystal phase and morphology of the samples and the transition process of the hydrothermal reaction. The content of La^{3+} in the samples was measured by inductively coupled plasma atomic emission spectroscopy. The photocatalytic activity of the La-doped TiO_2 (LaT) was measured under UV light with the degradation of methyl orange (MO, 10 mg/L). The results showed that the photocatalytic activity of TiO_2 was enhanced remarkably by La-doping. LaT hydrothermally prepared with 0.15 mol/L La^{3+} at under 180 °C showed the optimal reaction constant of 0.11 min^{-1} for the degradation of MO, about 9.20 and 3.69 times than those of bare TiO_2 and P25, respectively.

1. Introduction

Titania nanomaterials have attracted tremendous attention in the fields of photocatalysis and photoelectrochemistry [1–5]. Meanwhile, many studies have been performed on titanate functional materials, leading to the achievement of remarkable developments [6–9]. Layered titanate materials, such as $K_2Ti_4O_9$, $K_4Nb_6O_{17}$, and $K_2LaTi_3O_{10}$ [10,11], have extensive applications in photocatalysis. Their regular structure and designability show great potential for the adjustment of photo-reactivity on molecular and atomic levels. For example, modified $K_2La_2Ti_3O_{10}$ has shown better visible light absorption and superior photocatalytic activity for the degradation of organic dyes such as Rhodamine B. Furthermore, $K_2Ti_4O_9$ has also been used for NO_x storage, showing a high storage capacity [12,13].

Moreover, titanates have been recognized as useful precursors for the formation of TiO_2 [14–16]. When hydrothermally treated in alkali or acid solution, titanate readily transforms into TiO_2 of various morphology. When treated in HNO_3 solution with a pH of 2–7, $Na_2Ti_2O_5{\cdot}H_2O$ nanobars transform into anatase nanobars [17], the anatase grain size of which enlarges with increasing pH of the hydrothermal solution. It has been proposed that the H^+ ions in the solution exchange with Na^+ ions in the interlayers of the titanate [6], and the breakage and rearrangement of basic structural unit [TiO_6] octahedra leads to the formation of anatase nanocrystals. As the energy of the (001) facet is comparatively higher, the nanocrystal would grow along it to reduce the surface energy, leading to the formation of the anatase nanobars. Further works have shown

* Corresponding author. Tel: +86-21-64253056; Fax: +86-21-64252062; E-mail: fengchen@ecust.edu.cn
This work was supported by the National Nature Science Foundation of China (20777015) and the Innovation Program of Shanghai Municipal Education Commission (13ZZ042).
DOI: 10.1016/S1872-2067(11)60483-X | http://www.sciencedirect.com/science/journal/18722067 | Chin. J. Catal., Vol. 34, No. 3, March 2013

that the instability of titanates results from a large surface area, high amount of defects, and thin nanoplates, as well as poor rigidity, which are why it is able to transform to TiO_2 [18].

By pre-protonating, titanates can also be transformed into anatase when hydrothermally treated in neutral pH. Mao et al. [19] obtained anatase by hydrothermally treating protonated lepidocrocite type hydrogen titanate ($H_xTi_{2-x/4x/4}O_4$, x: ~0.7:vacancy) in pH 7 distilled water at 170 °C. Bavykin et al. [20] observed the crystal phase evolution of titanate ($Na_xH_{2-x}Ti_3O_7$) in various media including H_2O, 0.1 mol/L NaOH, 0.1 mol/L H_2SO_4, 0.1 mol/L HCl, and 0.1 mol/L HNO_3, by aging titanate at room temperature for 5 d to 5 months. The crystal phase of the titanate did not change after aging in water or 0.1 mol/L NaOH, but the titanate nanobars were decomposed, dissolved, and recrystallized into rutile TiO_2 of 3 nm in size with oval morphology when they were treated in acidic solutions. The author suggested that titanate nanobars stayed in a state of thermodynamic stability in alkali solution and in a dynamics stability state in acidic solution. Further, a lower crystallization rate was in favor of the formation of thermodynamically stable rutile with a symmetrical structure.

Titanates appear likely to transform into TiO_2 with special morphology under various conditions. Further, because the transformation process involves many factors, the transition mechanism from titanate to TiO_2 is still an issue. In addition, many works have proved that La-doped TiO_2 shows much better reactivity than blank samples [21,22]. Therefore, the introduction of La to a titanate system followed by hydrothermal treatment for the transition process would be a useful way to prepare La-doped TiO_2. In this paper, TiO_2 nanoparticles were prepared by treating titanate nanobars in acidic solution, and La^{3+} ions were introduced into the product to control the crystal phase and the photocatalytic performance of the as-prepared TiO_2. The photocatalytic activity of the samples was examined via the degradation of methyl orange (MO, 10 mg/L) under UV light. Finally, the mechanism of the transition process and the role of La^{3+} in enhancing the photocatalytic activity were proposed.

2. Experimental

2.1. Titanate preparation

Titanate nanorods ($K_2Ti_8O_{17}$) were synthesized using a similar method to that previously published [23]. A certain amount of P25 was dissolved into 70 ml KOH aqueous solution of 7 mol/L concentration, and the mixture was stirred for several min before it was transferred into an autoclave (100 ml) and treated at 180 °C for 72 h. After it had cooled to room temperature, the solid precipitate in the liner was centrifuged and washed with 0.01 mol/L hydrochloric acid and deionized water until the pH of the filtrate reached 7. The obtained white powder was dried at 80 °C in vacuum for 10 h and referred to as KTO.

2.2. Synthesis of La-doped TiO_2

The KTO (2.0 g) was mixed with 30 ml 0.1 mol/L HNO_3 with stirring for 30 min. Meanwhile, the desired amount of $La(NO_3)_3{\cdot}6H_2O$ (0–0.1 mol/L for 120 °C and 0–0.3 mol/L for 180 °C) was dissolved into 40 ml 0.1 mol/L HNO_3. The two solutions were then mixed together and hydrothermally treated at 120 °C (or 180 °C) for 48 h. According to the different hydrothermal temperature, the final obtained samples were referred to as LaT-120-x or LaT-180-x, where x stands for the concentration of La^{3+}; x = 0 corresponds to products prepared without La^{3+}.

2.3. Analysis and characterization

2.3.1. Catalyst characterization

The crystalline phase of the products was examined by powder X-ray diffraction (XRD) using a RIGAKU D/max2550 operating in reflection mode with a Siemens D5000 diffractometer (Cu K_α) at a scan rate of 0.02°/s. Scanning electron microscopy (SEM, JEOL JSM-6360LV) was used to examine the morphologies and particle size of the samples. Transmission electron microscopy (TEM) of the samples was carried out using a JEOL JEM 2100F operated at 200 kV. To prepare the TEM specimens, the powder samples were first ultrasonically dispersed in absolute ethanol and one or two drops of the suspension were the placed on a carbon film supported on a copper grid and dried in air before being transfer into the microscope. Inductively coupled plasma atomic emission spectroscopy (ICP-AES; TJA IRIS 1000) was used to measure the content of La element in the samples, for which the samples were dissolved in hydrogen fluoride (HF) solution before testing.

2.3.2. Photocatalytic activity

The UV photocatalytic activity of the composites was investigated for the photo-degradation of methyl orange (MO). UV irradiation was carried out using a 300 W high-pressure mercury lamp, which was surrounded by a quartz jacket to allow for water-cooling. An optical filter was used to cut off the light with wavelength longer than 390 nm to avoid the possible visible light induced dye photo-sensitized process. For a typical photocatalytic experiment, photocatalyst powder (0.10 g) was added to 100 ml aqueous MO (10 mg/L) solution; after adjusting the pH of the solution to ca. 4.0 with HCl or $NH_3{\cdot}H_2O$, the suspension was magnetically stirred in the dark for 30 min before UV illumination was conducted. The residual concentration of MO was then monitored by measuring its maximum absorbance with a UV-Vis spectrophotometer (Cary 100).

3. Results and discussion

3.1. Characterization of KTO

The XRD, TEM, HRTEM, and EDS results of KTO are shown in Figs. 1–3. The XRD pattern of the KTO matched well with previous reports [13] and the standard PDF of $K_2Ti_8O_{17}$ (JCPDS 80-2023, space group: C2/m(12)). However, the diffraction peak of the KTO (200) plane was shifted slightly from 11.33° to 10.80°. This may be ascribed to the intercalation of H_2O mole-

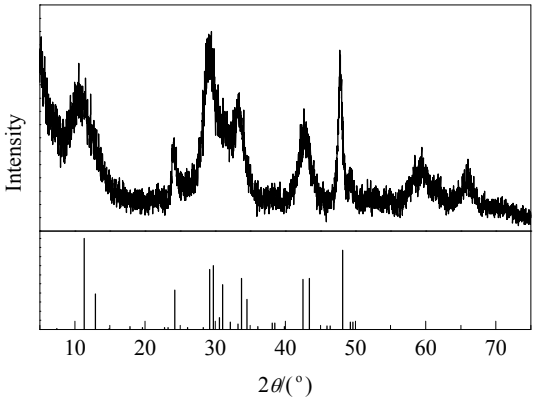

Fig. 1. XRD pattern of KTO product, the bar chart shows the standard XRD pattern of $K_2Ti_8O_{17}$ (JCPDS 80-2023).

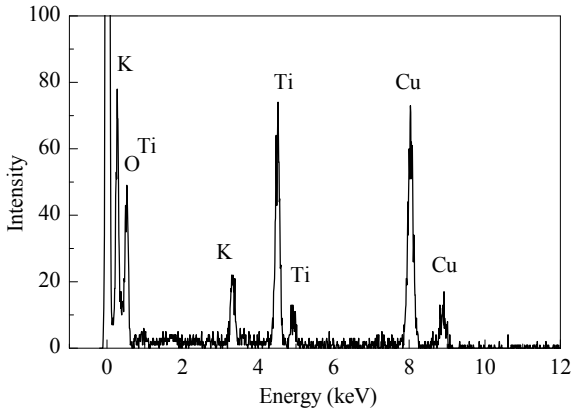

Fig. 2. EDS profile of KTO.

cules between the host layers of the titanate during the hydrothermal preparation, which slightly extended the layer space of the KTO. The peak shifted back to 11.33° after KTO was calcined (data not shown). Figure 2 shows the EDS spectra of KTO, from which the elemental molar fraction of K and Ti was calculated as 1:4, which verified its chemical formula of $K_2Ti_8O_{17}$. Figure 3 shows the TEM and HRTEM images of the KTO, respectively, which had a uniform nanobar morphology of ca. 100–150 nm length and ca. 15–20 nm width. The HRTEM image of KTO showed the layered structure of the samples; the nanobars grew along the [101] facet direction, and the interplanar spacing of the layers perpendicular to [101] was measured as 0.69 nm, consistent with that of (–201) of $K_2Ti_8O_{17}$. Because the interlayer spacing of (–201) is reported as 0.43 nm [24], while the radius of lanthanide series is within 0.085–0.105 nm, it was considered possible for La^{3+} to enter the interlayers of the obtained titanate.

3.2. Lattice evolution of products prepared with different hydrothermal temperatures and La^{3+} concentrations

Figure 4 shows XRD patterns of La^{3+}-doped samples obtained by hydrothermal treatment of KTO at 120 °C using various La^{3+} concentrations. When KTO was hydrothermally treated at 120 °C, the K^+ in the interlayers of the titanate exchanged with H^+ in the solution, and thus condensation between the basic units [TiO_6] was greatly promoted and led to a lattice rearrangement to the anatase structure, which is relatively similar to that of the titanate [25]. Particularly, the energy needed to transition into anatase is much lower than that into rutile; therefore, anatase was the dominant phase in the products. However, there was still some residual titanate in the La^{3+}-free sample (LaT-120-0), as shown in its XRD pattern (Fig. 4(1)). The introduction of La^{3+} appeared to promote the lattice transition, and complete lattice transition from titanate to anatase was observed for all La^{3+}-doped samples (Fig. 4(2)–(6)). Whatever the concentration of La^{3+} used, the LaT products were pure and highly crystallized anatase.

Figure 5 shows XRD patterns of La^{3+}-doped samples obtained by hydrothermal treatment of KTO at 180 °C using various La^{3+} concentrations. The La^{3+}-free sample (LaT-180-0) presented as a mixture of anatase and rutile. The transition process was more violent at 180 °C than that at 120 °C. Titanate and anatase have similar assemblies of octahedral [TiO_6] units, which each share four edges to form zigzag ribbon structures. Local dehydration occurs when layered titanate is hydrothermally treated in acid media, leading to rearrangement of local Ti–O–Ti bonds. The titanate transition to anatase generally progresses by rearrangement of lattice planes with shearing displacement along the (200) axis. Meanwhile, simultaneous lattice rearrangement in several directions is required when titanate transitions into rutile, which needs more energy [26]. Higher temperature and higher self-generated pressure provides adequate energy for the lattice transition to rutile, which accounts for the rutile phase observed in LaT-180-0, as shown

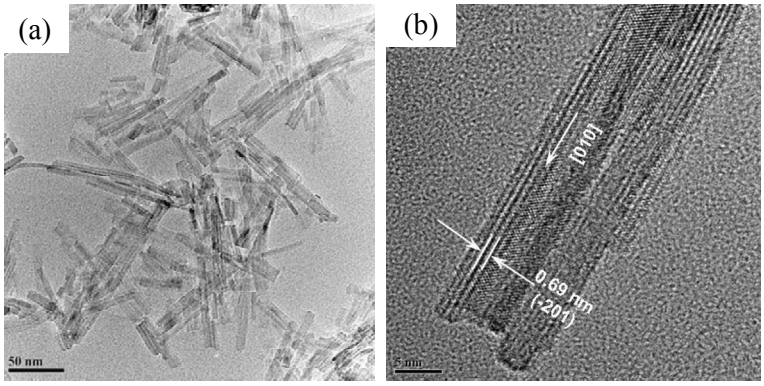

Fig. 3. TEM (a) and HRTEM (b) images of KTO.

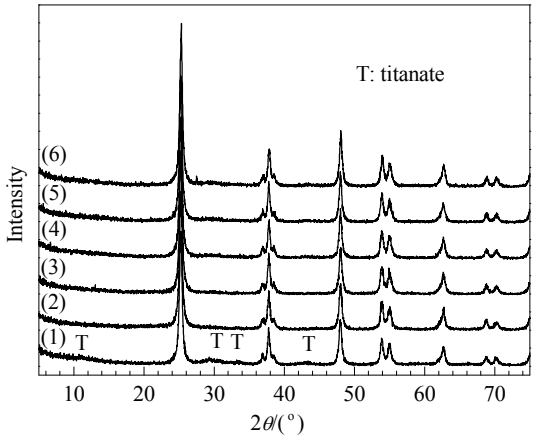

Fig. 4. XRD patterns of La^{3+}-doped samples obtained by acid hydrothermal treatment at 120 °C with various La^{3+} concentrations. (1) LaT-120-0; (2) LaT-120-0.001; (3) LaT-120-0.003; (4) LaT-120-0.005; (5) LaT-120-0.01; (6) LaT-120-0.1

in Fig. 5(1). The introduction of La^{3+} suppressed the transition from titanate into rutile; although an anatase and rutile mixture was obtained for the La^{3+}-free product (LaT-180-0), only pure anatase was observed in products prepared in the presence of La^{3+}.

TEM images of the La^{3+} doped samples are shown in Fig. 6. KTO presented typical nanobar morphology. After hydrothermal treatment in 0.1 mol/L HNO_3 at 120 °C, most of the nanobars ruptured to form nanoparticles, and consequently LaT-120-0 showed a mixture of nanobars and nanoparticles. According to the XRD patterns, it was obvious that the nanobars were titanate in phase and there nanoparticles were anatase phase. Increasing the temperature to 180 °C promotes the morphological transition, and the TEM image of LaT-180-0 only exhibited nanoparticle-like morphology, as shown in Fig. 6(c). The morphology evolution process is actually induced by phase transition of titanate into TiO_2. As shown, the XRD pattern of LaT-180-0 exhibited typical signals of an anatase/rutile mixture. When La^{3+} was introduced into the hydrothermal media, the morphology of products LaT-120-0.005 (Fig. 6(d)) and LaT-180-0.1 (Fig. 6(e)) was quite similar to that of sample LaT-180-0. The anatase grains (see XRD patterns in Figs. 4 and 5) observed were typical anisotropic nanoparticles with regular geometric shape, but not spheres. Their highly regular crystal morphology suggested that the obtained anatase was highly crystalline and thus may have good photocatalytic performance. The average grain sizes of the prepared LaTs were calculated with the Scherrer equation [27]:

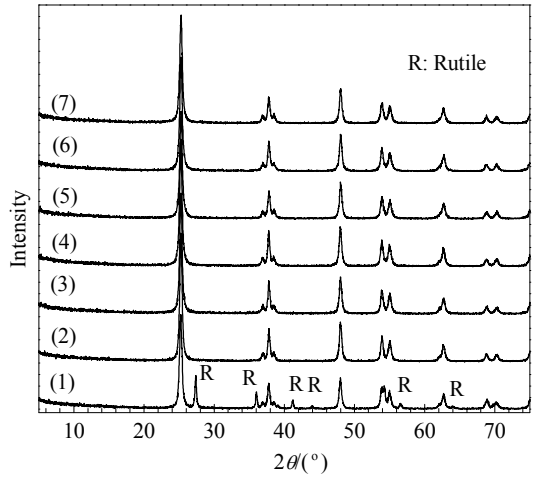

Fig. 5. XRD patterns of La^{3+}-doped samples obtained by acidic hydrothermal treatment at 180 °C with various La^{3+} concentrations. (1) LaT-180-0; (2) LaT-180-0.005; (3) LaT-180-0.01; (4) LaT-180-0.1; (5) LaT-180-0.15; (6) LaT-180-0.2; (7) LaT-180-0.3.

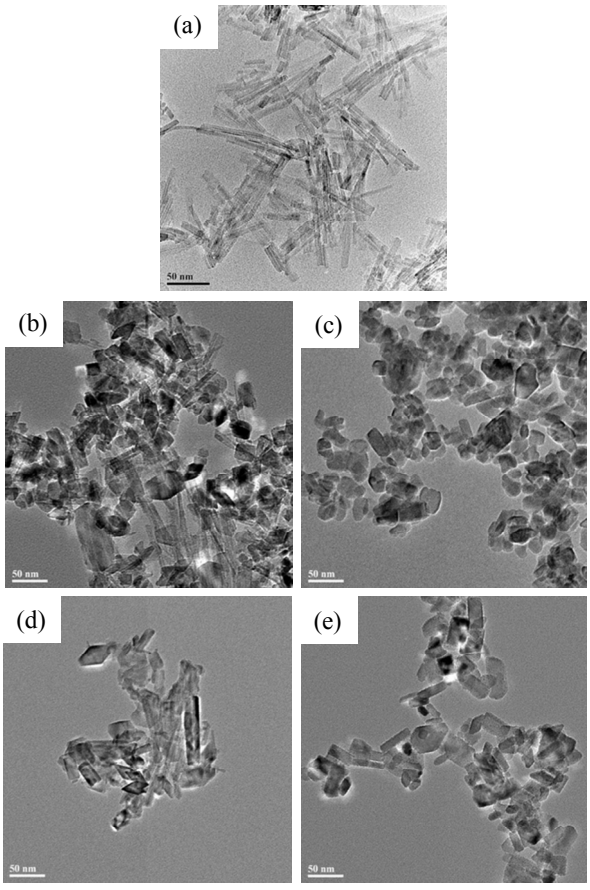

Fig. 6. TEM images of KTO (a), LaT-120-0 (b), LaT-180-0 (c), LaT-120-0.005 (d), and LaT-180-0.1 (e).

$$D = K\lambda/\beta\cos\theta$$

where β is the half-height width of the anatase diffraction peak, K is a coefficient of 0.89, θ is the diffraction angle, and is the X-ray wavelength corresponding to Cu K_α radiation. The results are listed in Table 1. The raised hydrothermal temperature significantly increased the grain size of the anatase, while the introduction of La^{3+} little changed the size little. The content of La in each sample, as tested by ICP-AES, is also shown in Table 1. The data show that the actual La content (wt%) in the LaT-120-*x* samples was comparatively higher than that in LaT-180-*x* samples when the same La^{3+} concentration was used in the preparation of the TiO_2. Most probably, as the La^{3+} ion has lower solubility at lower hydrothermal temperature, it was easier for it to form oxide clusters on the surface of the catalyst rather than embed in isolation. At higher hydrothermal temperature, La^{3+} ions were more disassociated into the aqueous

Table 1
Calculated average anatase grain size and La content of LaT samples.

Sample	Grain size [a] (nm)	Content of La [b] (wt%)
LaT-120-0	19.1	0
LaT-120-0.001	18.5	0.025
LaT-120-0.003	19.0	0.048
LaT-120-0.005	19.3	0.27
LaT-120-0.01	19.8	0.31
LaT-120-0.1	19.6	1.6
LaT-180-0	23.6	0
LaT-180-0.005	24.6	0.014
LaT-180-0.01	23.9	0.067
LaT-180-0.1	24.4	0.18
LaT-180-0.15	22.1	0.19
LaT-180-0.2	22.4	0.27

[a] Calculated by Scherrer equation.
[b] Tested by ICP-AES.

solution and less embedded into the TiO_2. Notably, La^{3+} ions were likely more effectively dispersed (but not in the form of oxide clusters) when embedded into the TiO_2 at higher hydrothermal temperature, thus resulting in better photocatalytic performance (as shown in section 3.5).

3.3. *Effect of proton on the lattice transition*

The results above show that KTO, that is $K_2Ti_8O_{17}$, was able to transform into TiO_2 via hydrothermal treatment at pH 1.0. Presumably, the loss of K^+ and dehydration by hydroxyl condensation was the key step in the lattice transition process. Hence, the KTO was also hydrothermally treated with La^{3+} at 120 °C at pH 4.0 (using 0.1 mmol/L HNO_3), which contains much fewer H^+ ions as compared with pH 1.0. The XRD patterns of the as-obtained samples are presented in Fig. 7, which shows that the titanate structure was still remaining in the as-obtained samples (Fig. 7(1) and (2)). Compared with that occurring at pH 1.0, the transition procedure from titanate to TiO_2 at pH 4.0 was definitely restrained. This result indicated that a sufficient amount of H^+ is indispensable for the lattice

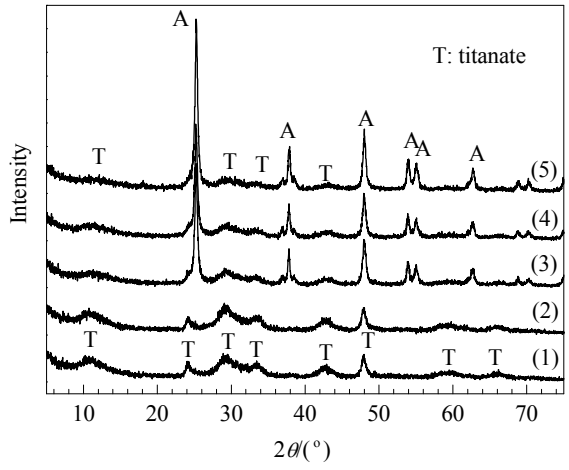

Fig. 7. XRD patterns of hydrothermally treated KTO with 0.01 mol/L La^{3+} (1), 0.005 mol/L La^{3+} (2), hydrothermally treated H^+ pre-exchanged KTO with 0.0025 mol/L La^{3+} (3), 0.005 mol/L La^{3+} (4), and 0.1 mol/L La^{3+} (5). Hydrothermal conditions: 120 °C, pH 4.0.

transition process. During the hydrothermal treatment, H^+ exchanged with K^+ in the interlayer, forming hydrogen titanate, which is much easier to dehydrate during the transition to anatase.

K^+ deprivation can be partly achieved with careful H^+ pre-exchange treatment in acidic solution. It has been reported that $Na_2Ti_2O_5{\cdot}H_2O$ transforms into hydrogen dititanate when washed with acid [28], and hydrogen dititanate readily transforms into TiO_2 upon hydrothermal or thermal treatment. Therefore, a pre-treating method was carried out. In a typical procedure, 2.0 g KTO was dispersed in 64 ml HNO_3 (pH 1.0) for 0.5 h, then filtered and hydrothermally treated with La^{3+} at 120 °C and pH 4.0. Figure 7(3)–(5) shows XRD patterns of the products of H^+ pre-exchanged KTO hydrothermally treated with 0.0025, 0.005, and 0.1 mol/L La^{3+}, respectively.

Compared with samples that did not undergo the H^+ pre-exchange procedure (Fig. 7(1) and (2)), the amount of titanate phase in the samples prepared with the H^+ pre-exchange procedure decreased to a very low level while the anatase content greatly increased. The H^+ ions play a dominant role in the lattice transition. H^+ ions exchange with K^+ ions in the titanate interlayer, and then carry out a dehydration procedure to initiate the merging of the two host layers to form TiO_2 under hydrothermal treatment. Although the H^+ pre-exchange procedure greatly aided the removal of K^+ from the interlayers, complete K^+ deprivation appeared to only be achieved by hydrothermal treatment, because ion-exchange is promoted under hydrothermal conditions.

3.4. *Schematic illustration of the transition process*

A schematic illustration of the transition process from KTO to titania for different procedures is shown in Fig. 8. When hydrothermally treated in HNO_3 solution of pH 1, the large amounts of H^+ in the solution readily exchange with K^+ in the interlayers of the titanate to form protonated titanate (HTO) instead of KTO. HTO is a more metastable phase and tends to undergo a dehydration process to transition into anatase. However, at pH 4.0, the much lower H^+ concentration leads to insufficient exchange between K^+ and H^+, which means that most K^+ ions remain in the interlayers of the titanate, thus

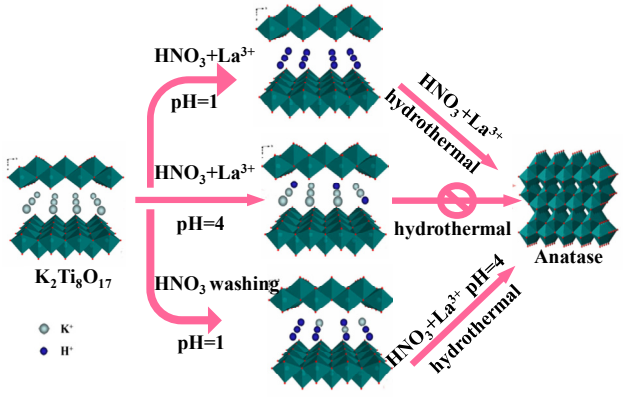

Fig. 8. Schematic illustration of the transition process from KTO to titania for different procedures.

making it difficult to transform from KTO to TiO_2. A H^+ pre-exchange process greatly helps to remove the K^+ in the interlayers. Thus, when treated in HNO_3 solution at pH 1, K^+ in the interlayers of KTO exchanges with the high concentration of H^+, and a similar dehydration process occurs to produce anatase phase TiO_2 under the subsequent hydrothermal treatment. However, the ion-exchange ability of the H^+ pre-exchange process occurring at room temperature is much weaker than that under hydrothermal treatment (at 120 and 180 °C), and thus the products obtained in this way (Fig. 7(3)–(5)) were universally a mixture of anatase and a small amount of titanate, i.e., KTO did not completely transition to TiO_2.

3.5. *Photocatalytic activity of La-doped TiO_2*

The process of MO degradation of the samples to MO appeared to follow apparent first-order kinetics. The photocatalytic degradation of MO with various LaT-120-*x* samples and the corresponding MO degradation reaction constants for the various La^{3+} concentrations used are shown in Fig. 9 and Table 2. The degradation rates differed widely with La^{3+} concentration. It is clear that the degradation rates of most of the La-doped samples, except those with a too great La^{3+} concentration (i.e. 0.01 and 0.1), were greatly enhanced by La^{3+} doping (Fig. 9). The MO degradation reaction constants increased obviously when the La^{3+} concentration was increased from 0 to 0.003 mol/L, while it decreased when the concentration was increased from 0.003 to 0.1 mol/L, with optimal activity at 0.003 mol/L (Table 2). Notably, all LaT-120-*x* samples except

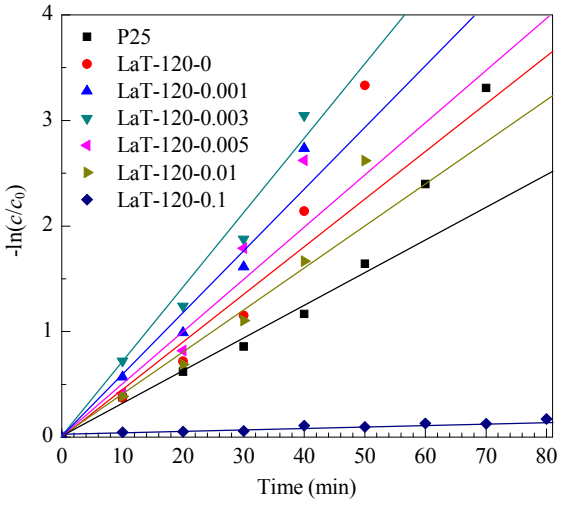

Fig. 9. Photocatalytic degradation of MO over LaT-120-*x* samples and P25 TiO_2 under UV irradiation.

Table 2
The degradation reaction constant of MO vs. La^{3+} concentration used in the hydrothermal preparation of LaT-120-*x* samples.

Concentraion of La^{3+} (mol/L)	k/min^{-1}
0	0.038
0.001	0.054
0.003	0.063
0.005	0.060
0.01	0.037
0.1	0.002

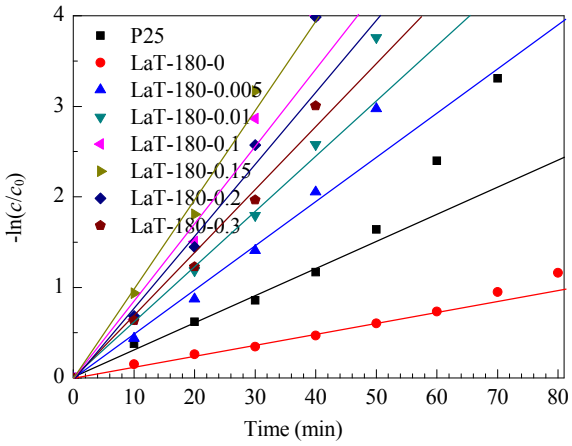

Fig. 10. Photocatalytic degradation of MO over LaT-180-*x* samples and P25 TiO_2 under UV irradiation.

Table 3
The degradation reaction constant of MO vs. La^{3+} concentration used for the hydrothermal preparation of the LaT-180-*x* samples.

Concentraion of La^{3+} (mol/L)	k/min^{-1}
0	0.011
0.005	0.047
0.01	0.060
0.1	0.096
0.15	0.106
0.2	0.086
0.3	0.065

that with 0.1 mol/L La^{3+} showed much higher MO degradation reaction constants than that of P25. Particularly, the MO degradation reaction constant of LaT-120-0.003 (0.063 min^{-1}), the optimal, was almost 2.19 times that of P25 (0.028 min^{-1}). Therefore, the addition of La^{3+} in this work not only promoted the transition process from titanate to anatase (as shown by XRD), but also improved the separation of photogenerated electrons and holes which largely contribute to enhance the photoactivity. Under hydrothermal treatment, La^{3+} likely combined onto the surface of the TiO_2 and may even have occupied surface defects, thus improving carrier separation during the photocatalytic process to enhance the activity of the photocatalysts. However, when the La^{3+} concentration of was excessively high, the over-enriched La^{3+} likely form additional metal oxide clusters, which normally act as recombination centers for photogenerated electrons and holes, thus reducing the photocatalytic activity of the TiO_2.

The photodegradation of MO with various LaT-180-*x* (Fig. 10) samples and the corresponding MO degradation reaction constant with La^{3+} concentration used (Table 3) were also investigated. Degradation rates for all La^{3+} doped significantly exceeded those of P25 and the La^{3+}-free sample LaT-180-0, which means that La-doping had an obviously positive effect on the photocatalytic activity of the samples. Table 3 shows the relationship of MO degradation reaction constant to La^{3+} concentration. When La^{3+} concentration was increased from 0 to 0.15 mol/L, the reaction constants also significantly increased before decreasing when the La^{3+} concentration was further increased from 0.15 to 0.3 mol/L. The reaction constants of all

Graphical Abstract

Chin. J. Catal., 2013, 34: 585–592 doi: 10.1016/S1872-2067(11)60483-X

La-doped titania nanocrystals with superior photocatalytic activity prepared by hydrothermal method

JIAO Yanchao, ZHU Mingfeng, CHEN Feng*, ZHANG Jinlong
East China University of Science and Technology

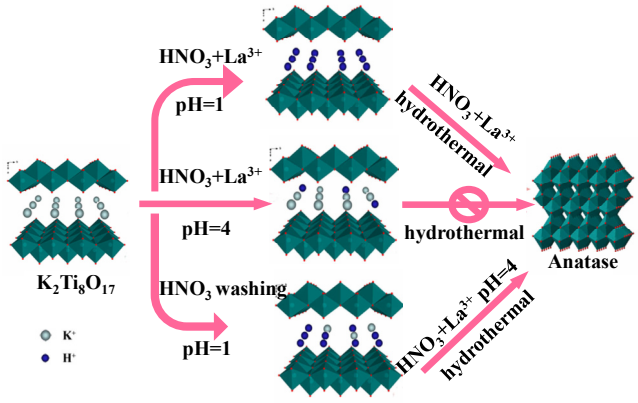

La^{3+} doped TiO_2 was prepared by treating $K_2Ti_8O_{17}$ in acidic solution. TiO_2 doped with 0.15 mol/L La^{3+} gave the optimal reaction constant of 0.11 min^{-1} for methyl orange degradation, about 9.20 times that of bare TiO_2.

La-doped samples were much larger than those of the La^{3+}-free sample (LaT-180-0) and P25. The optimal reaction constant at 0.15 mol/L La^{3+} (0.11 min^{-1}) was about 9.20 times greater than that of LaT-180-0 and 3.69 times greater than that of P25 (0.029 min^{-1}). Besides promoting the separation of photogenerated electrons and holes, the La^{3+} restrained the transition of titanate into rutile to induce the formation of pure anatase (as shown by XRD), likely also significantly contributed to the enhanced photocatalytic activity of the LaT-180-*x* samples.

4. Conclusions

The photodegradation of MO with various LaT-180-*x* (Fig. 10(a)) samples and the corresponding MO degradation reaction constant with La^{3+} concentration used (Fig. 10(b)) were also investigated. Degradation rates for all La^{3+} doped significantly exceeded those of P25 and the La^{3+}-free sample LaT-180-0, which means that La-doping had an obviously positive effect on the photocatalytic activity of the samples. Figure 10(b) shows the relationship of MO degradation reaction constant to La^{3+} concentration. When La^{3+} concentration was increased from 0 to 0.15 mol/L, the reaction constants also significantly increased before decreasing when the La^{3+} concentration was further increased from 0.15 to 0.3 mol/L. The reaction constants of all La-doped samples were much larger than those of the La^{3+}-free sample (LaT-180-0) and P25. The optimal reaction constant at 0.15 mol/L La^{3+} (0.11 min^{-1}) was about 9.20 times greater than that of LaT-180-0 and 3.69 times greater than that of P25 (0.029 min^{-1}). Besides promoting the separation of photogenerated electrons and holes, the La^{3+} restrained the transition of titanate into rutile to induce the formation of pure anatase (as shown by XRD), likely also significantly contributed to the enhanced photocatalytic activity of the LaT-180-*x* samples.

References

[1] Fujishima A, Honda K. *Nature*, 1972, 37: 238
[2] Fujishima A, Rao T N, Tryk D A. *J Photochem Photobiol C*, 2000, 1: 1
[3] Mahmood T, Wang X S, Chen C C, Ma W H, Zhao J C. *Chin J Catal*, 2007, 28: 1117
[4] Li H X, Zhu J. *Chin J Catal*, 2008, 29: 91
[5] Chen X B. *Chin J Catal*, 2009, 30: 839
[6] Li N, Zhang L D, Chen Y Z, Fang M, Zhang J X, Wang H M. *Adv Funct Mater*, 2012, 22: 835
[7] Qian D N, Xu B, Cho H M, Hatsukade T, Carroll K J, Meng Y S. *Chem Mater*, 2012, 24: 2744
[8] Xiao M, Wang X, Zhang Q Q, Ding H M. *Chin J Inorg Chem*, 2012, 28: 1743
[9] Lu R, Jiang G S, Li B, Zhao Q L, Zhang D Q, Yuan J, Cao M S. *Chin Phys Lett*, 2012, 29: 058101
[10] Huang Y, Wu J, Li T, Hao S, Lin J. *J Porous Mater*, 2006, 13: 55
[11] Cui W Q, Qi Y L, Hu J S, Liu L, Liang Y H. *Acta Chim Sin*, 2012, 70: 691
[12] Kumar V, Govind, Uma S. *J Hazard Mater*, 2011, 189: 502
[13] Shen W H, Nitta A, Chen Z, Eda T, Yoshida A, Naito S. *J Catal*, 2011, 280: 161
[14] Zhao B, Chen F, Huang Q, Zhang J. *Chem Commun*, 2009: 5115
[15] Zhao B, Chen F, Jiao Y, Yang H, Zhang J. *J Mol Catal A*, 2011, 348: 114
[16] Jiao Y, Zhao B, Chen F, Zhang J. *CrystEngComm*, 2011, 13: 4167
[17] Nian J N, Teng H. *J Phys Chem B*, 2006, 110: 4193
[18] Zhu H Y, Lan Y, Gao X P, Ringer S P, Zheng Z F, Song D Y, Zhao J C. *J Am Chem Soc*, 2005, 127: 6730
[19] Mao Y B, Wong S S. *J Am Chem Soc*, 2006, 128: 8217
[20] Bavykin D V, Friedrich J M, Lapkin A A, Walsh F C. *Chem Mater*, 2006, 18: 1124
[21] Zhao Q H, Quan X J, Tan H Q, Sang X M. *Chin J Catal*, 2008, 29: 269
[22] Wei W, Dai Y, Guo M, Yu L, Huang B B. *J Phys Chem C*, 2009, 113: 15046
[23] Kasuga T, Hiramatsu M, Hoson A, Sekino T, Niihara K. *Adv Mater*, 1999, 11: 1307
[24] Cao J C, Wang A L, Yin H B, Shen L Q, Ren M, Han S Q, Shen Y T, Yu L B, Jiang T S. *Ind Eng Chem Res*, 2010, 49: 9128
[25] Li J G, Ishigaki T, Sun X. *J Phys Chem C*, 2007, 111: 4969
[26] Xu J S, Zhang H, Li W B, Zhang J, Liu X Y, He X K, Xu D L, Qian J H, Liu L. *Micro Nano Lett*, 2012, 7: 654
[27] Wu Y, Liu H, Zhang J, Chen F. *J Phys Chem C*, 2009, 113: 14689
[28] Tsai C-C, Teng H. *Chem Mater*, 2006, 18: 367